

# A Study on Flood Hazard Zonation Mapping Based on GIS-Driven Approach Using Remote Sensing Data and Weighted Overlay Analysis (WOA) Model

**Kamuju Narasayya**

Scientist, CWPRS

## Abstract

Flood hazard mapping is crucial for identifying flood-prone areas and developing effective mitigation strategies. This study utilized a Weighted Overlay Analysis, which is one of the subjective model derived from Multi-Criteria Decision Support System (MCDA), to assess flood hazards in the Auranga watershed, India. Six key flood-inducing factors were selected, including topographic data such as elevation, slope, river distance, and flow length derived from remote sensing data of Digital Elevation Model and classified Land use/Land cover data, along with hydro-meteorological data of precipitation. Each dataset was standardized to a common scale to facilitate comparison and integration. Weights were assigned to the layers like elevation, slope, river distance, flow length, Land use/Land cover, and precipitation according to their significance in contributing to flood risk. These weighted layers were then combined using GIS tools like ArcGIS, resulting in a composite map that delineates areas with varying flood hazard zones. The final flood hazard map identified that approximately 914 sq. km (60.0%) of the study area was at high to very high flood risk, particularly in regions close to rivers, while around 97 sq. km (6.4%) exhibited very low flood hazard. The GIS-Weighted Overlay Analysis method proved effective in flood hazard zone mapping, especially when incorporating a greater number of parameters. This approach is widely recognized in environmental planning and risk assessment, especially in areas vulnerable to natural disasters like floods.

**Keywords:** Flood Hazard, Geographic Information System, Weighted Overlay Analysis, Digital Elevation Model, Euclidian Distance

## 1. Introduction

Floods are among the most devastating natural disasters, causing extensive and often irreversible damage to property and communication infrastructure. This destruction results in significant loss of human and animal life, as well as the loss of agricultural produce and farmland. While modern technology and information systems have improved our ability to monitor and manage these disasters, the impact of floods remains severe. Despite their destructive nature, floods can have some beneficial effects, such as transporting fertile soil to farmlands and distributing fish to smaller water bodies. However, the overall consequences are typically far more harmful. Floodwaters often become contaminated, leading to the spread of various diseases, including cholera, typhoid fever, leptospirosis, hepatitis A, malaria, and

dengue. These health risks further exacerbate the challenges faced by affected communities. Flood mapping can support in decision-making for such events by facilitating risk management, near real-time forecasting, and Land Use and Land Cover management. Floods are multi-dimensional dynamic phenomena thus, Geographic Information System (GIS)/Remote Sensing (RS) data have been largely delineated to explore the extent of flooded areas. Near real-time flood monitoring is essential to mitigate floods and thus control their impact [1]. Sofia et al. [2] found that cumulative flood hazard delineation along with environmental degradation and climate change parameters associated with LandUse/LandCover changes can ensure better monitoring capability. The pixel-based flood analysis requires huge time and processing capabilities to achieve near real-time assessment.

Flood vulnerability combines inundation extent with social data, which is used to determine flood-prone communities that have the greatest propensity for loss of property and life. Currently, flood exposure and vulnerability are mapped using hydrodynamic inundation models along with high-resolution population distribution data in developed countries with high population density [3]. Flood susceptibility mapping uses analysis techniques, such as multi-criteria decision analysis [4], logistic regression [5], frequency ratio approach [6], weight of evidences equations [7], k-nearest neighbor logic [8], analytic network process framework [9], Bayesian network fusion technique [10], hydraulic modeling used for estimating unsaturated soil hydraulic conductivity [11], and soil water assessment tool (SWAT) in the ArcGIS software environment [12] are some models utilized for flood susceptibility estimation. Deep learning methods, such as artificial neural networks (ANNs), fuzzy logic, support vector machines, random forest classification, regression trees (RTs), and classification and RT (CART) algorithms (13-15) have significant potential for effective flood mapping and monitoring. ANN has been extensively used for flood susceptibility mapping [16,17], however, it has drawbacks, such as over-fitting and under-fitting, slow learning, the curse of dimensionality, and slow convergence to a local optimum in addition, its performance for processing complex hydrological phenomena has been inadequate [18-19]. Tellman et al. [20] proposed a new approach for flood modeling by leveraging satellite images with a cloud computing-enabled Google Earth Engine (GEE) system to map flood hazards in real time in two ways: First, by generating a globally consistent flood inundation layer, and second, by dynamically modeling flood susceptible areas. A cloud computing GEE-based flood prevention and emergency response system (FPERS) has been successfully developed and implemented for three frontal applications of before, after, and during floods occurring during typhoons or torrential rain events in China from 2013 to 2016 [21]. Climate change is playing a vital role in inducing the extreme rainfall which is visible in the recent decades. Climate model simulations and empirical evidence confirm that warming climates owing to increased water vapor lead to more instance precipitation events and therefore increase risks of floods [22,23]. Flood hazard mapping is a significant component for policy planners to identify the areas which are vulnerable to floods. Furthermore, flood hazard zone mapping will be significantly important for urban planning and risk management.

### ***1.1 Scope and Objectives***

Conventional flood mapping was carried out using few parameters because of slow image processing systems and complex ranking of susceptibility levels of the parameters. In some cases, flood susceptibility mapping parameters were limited to topographic parameters. Six major flood hazard mapping criteria were identified, namely topographic, and hydro-meteorological interference criteria, which include 6 sub-criteria, for intelligent assessment and flood susceptibility mapping.

### 1.2 Flood Hazard Mapping Parameters

Basic parameters, such as precipitation, and topographical variations, such as elevation, slope river distance, flow length, and Land Use Land Cover, were measured and evaluated for identifying flood-causing factors at river banks [24]. A higher precipitation rate considerably increases the probability of floods in a flood-prone area, along with contribution from other parameters. High river network density in a region implies accelerated surface runoff and increases the possibility of flooding [25]. LU/LC dynamics parameters affect hydrological processes components, such as infiltration, surface runoff, evaporation, and evapotranspiration [26]. In another study, LU/LC dynamics along with elevation and slope were considered factors that had the most significant effect on flooding in a region [27].

## 2. Materials and Methodology

### 2.1 Study Area

The present study was carried out in the ‘Auranga’ watershed (Watershed code: C2ASON01 to 83 as per India-WRIS watershed atlas) of son sub-basin of Ganga basin covered in Latehar district of Jharkhand state of India. The main river flows in this watershed is ‘Auranga’ river in Latehar and Palamu districts, therefore, the name of watershed titled as ‘Auranga’ watershed. The ‘Auranga’ river has two principle tributaries of Sukri, Ghaghri, till it flow into the ‘Koel’ near Kechki 16 km south of Daltonganj. The watershed covers a total geographical area of 1520 km<sup>2</sup> lies between 23<sup>0</sup>39’4’’N latitude and 83<sup>0</sup>39’20’’E longitude to 23<sup>0</sup>23’43’’N latitude and 84<sup>0</sup>46’32’’E longitude with an average elevation of 784m above mean sea level altitude as shown in Fig.1. The average annual rainfall in the ‘Auranga’ watershed was noted as 819 mm from 2004 to 2008. The ‘Auranga’ river rises near Saheda in pass leading down from the Chhtanagpur plateau. The riverbed is very rocky in some places and sandy above the junction with the orth Koel. Like the North Koel it carries a large volume of water in rains but the summer dries up completely.

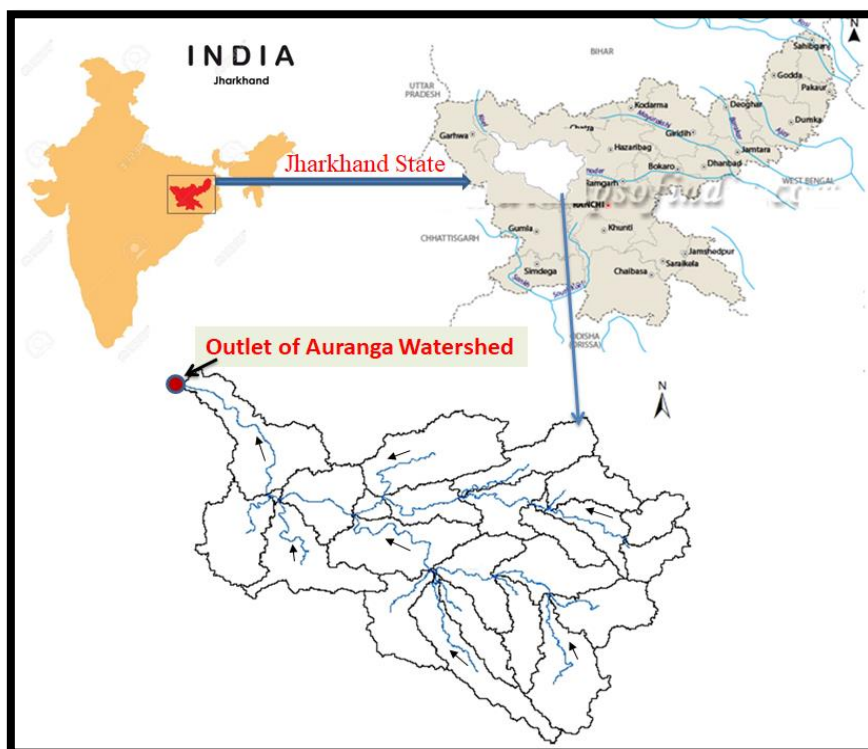


Fig. 1: Location Map of Study area - ‘Auranga’ Watershed

**2.2 Data and Data Source**

Open source spatial data for the study area and secondary information from several sources such as SRTM, IMD and GlobCover for flood hazard mapping (Table:1). Through an extensive literature review and expert opinions, six main criteria were selected for flood hazard mapping.

**2.3 Methodology**

The study focused on flood hazard mapping by utilizing various datasets and following a systematic sequence of methods. The research aimed to develop a Weighted Overlay Analysis (WOA) model, integrating Remote Sensing and GIS techniques within a geospatial environment using ArcGIS 10.8.1. The model

S.N	Data Type	Description	Source
1	DEM	ASTER DEM (30 m)	<a href="https://www.earthdata.nasa.gov">https://www.earthdata.nasa.gov</a>
2	Precipitation	IMD-India	<a href="https://www.imdpune.gov.in/cmpg/Griddata/Rainfall_25_NetCDF.html">https://www.imdpune.gov.in/cmpg/Griddata/Rainfall_25_NetCDF.html</a>
3	Land use Land cover	GlobCover	<a href="http://due.esrin.esa.int/page_globcover.php">http://due.esrin.esa.int/page_globcover.php</a>

**Table 1. Description of data sources used for processing flood hazard mapping criteria**

was constructed using six key flood-influencing physical variables: elevation, slope, rainfall, LandUse/LandCover (LU/LC), distance from rivers, and flow length. The primary objective was to create a flood hazard zone map that categorizes areas into very high, high, moderate, low, and very low flood hazard zones. The study employed a Multi-Criteria Decision-Making (MCDM) approach, specifically the Weighted Overlay Analysis, to calculate the relative importance of each factor, ensuring an accurate and meaningful outcome [28]. The MCDM-based WOA model effectively quantified the weightage of the six selected factors, helping to determine the potential of each element in contributing to flood hazards. The detailed discussion on this process is provided below. The methodology applied as shown in flow chart [Fig.2]

**2.4 Weighted Overlay Analysis (WOA) Model**

WOA is one of the method derived from a Multi-Criteria Decision Making (MCDM) approach. The concept of Weighted Overlay Analysis (WOA) for flood hazard mapping has been developed and refined by various researchers over time. One of the key contributors to the development of this method is Thomas. This method laid the groundwork for WOA by providing a systematic approach to assigning weights to different factors. Weighted Overlay Analysis is a widely used method in Geographic Information Systems (GIS) for combining multiple spatial datasets to assess and map different scenarios, such as flood vulnerability, land suitability, and environmental risk. This approach is particularly effective in situations where multiple factors contribute to a certain outcome, and it helps to determine the relative importance (or weight) of each factor.

The Weighted Overlay Analysis is a decision support tool used to determine the weights and ranks of various parameters for identifying flood-vulnerable zones (FVZ). In this study, the WOA model was

developed using six thematic layers, which were applied to categorize different flood hazard zones. The model assigns varied weights to each parameter based on its relative importance in contributing to flood risk. This can be done through expert judgment, statistical analysis, or a combination of both. Table 3 provides the specific weightage assigned to each variable in the analysis.

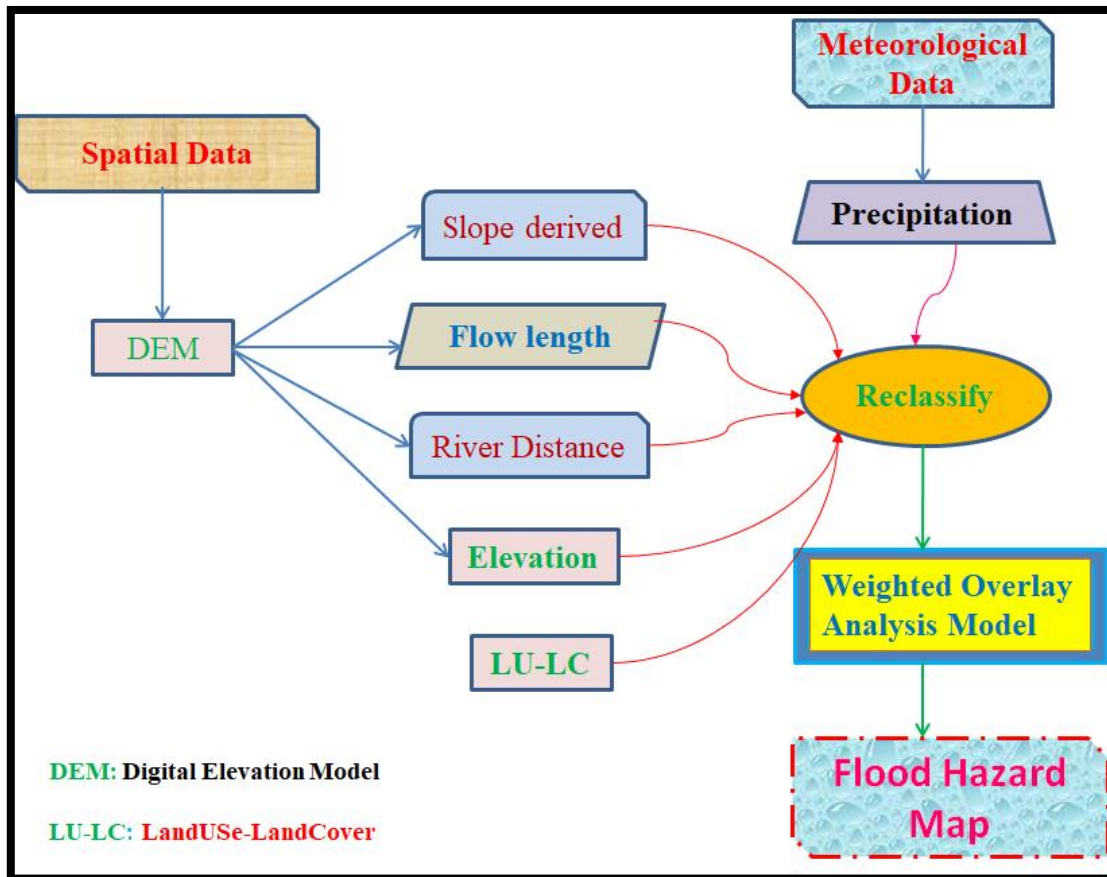


**Figure 2: Flow chart of methodology**

Identifying and selecting the relevant factors or criteria that influence the outcome. For flood hazard mapping, these might include elevation, slope, land use/land cover, distance from rivers, precipitation, flow length etc. The weighted criteria are combined using GIS tools, resulting in a composite map that reflects the overall scenario (e.g., flood hazard zones). The final map highlights flood areas of very high, high, moderate, low and very low risk zones.

The specific application of WOA in GIS is a result of integrating these MCDM principles with spatial analysis capabilities, particularly through software like ArcGIS developed by Esri. The methodologies were further refined by various researchers and practitioners in the field of environmental science, urban planning, and disaster management. For modern GIS-based WOA, Esri's development of tools within the ArcGIS environment has been instrumental in popularizing and standardizing the approach. However, no single individual is credited with inventing WOA in its GIS application; it is an evolution of MCDM principles applied within the context of spatial analysis.



**Table 3: Numerical weightage of each variable**

Name of variable	Weightage
Slope	40
Flow length	5
Precipitation	15
River distance	5
LU/LC	5
Elevation	30

### 3. WOA Model Influencing Factors

The WOA model is influenced by six key factors: watershed slope, stream flow length, precipitation grid data, river proximity, land use/land cover, and topographic elevation within the watershed. Each of these factors plays a significant role and is described in detail below.

#### 3.1 Slope

In the hydrological study, slope plays a vital role to regulate the flow of surface water, and it is one of the most important topographic factors for such studies [29, 30]. Land surface slope is one of the effective factors in floods lower the slope higher is the intensity of flood and the higher the slope lower is the intensity of flood occurrence. The slope of a channel in a region is having a direct relationship with the flow velocity [30]. When the river slope increases then the flow velocity in the river also will increase [31]. The slope has a direct relation to infiltration. An increase of the surface slope reduces the infiltration process but increases the surface runoff; as a result, in the regions having a lower surface slope, an enormous volume of water becomes stagnant and causes a flood situation. The slope map has been created from the Shuttle Radar Topographic Mission (SRTM) Digital Elevation Model (DEM) 30 m resolution and reclassified as shown in [figure 3](#).

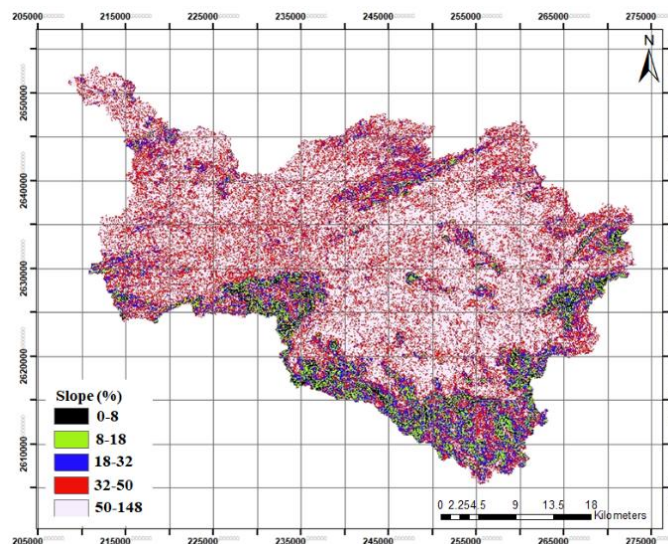


**Figure 3: Reclassified slope Map**

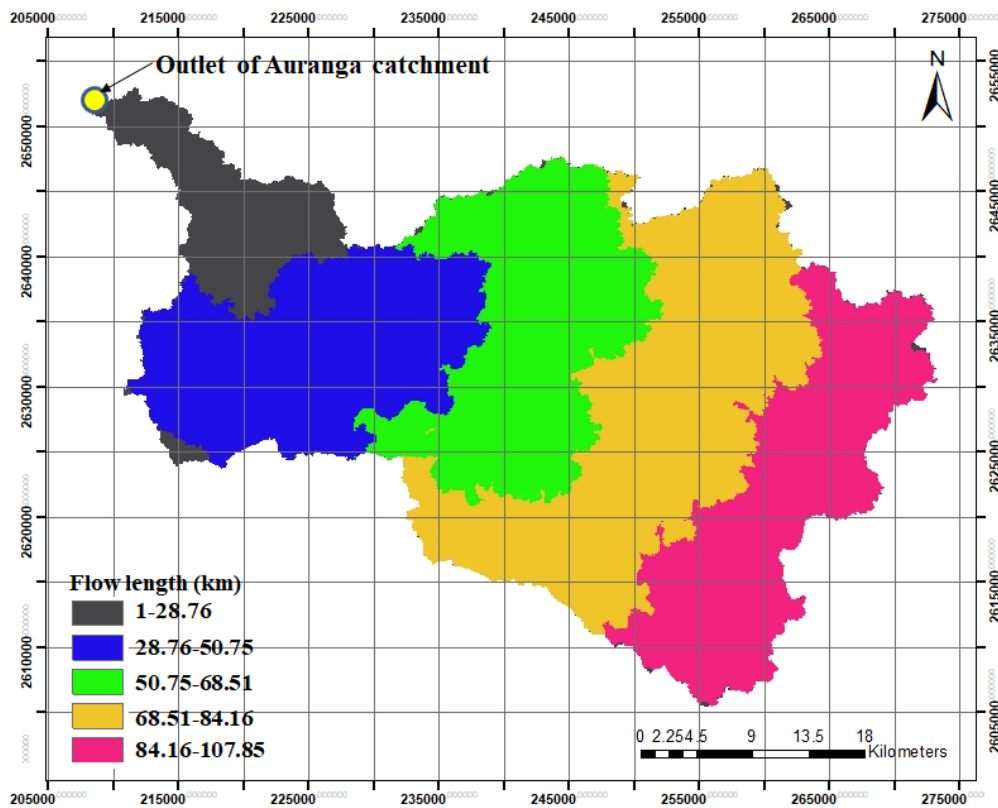


**Figure 4: Reclassified Flow length Map**

### 3.2 Flow Length

Flow length is a key criterion in flood hazard mapping, representing the distance that water travels from a point on the terrain to the nearest drainage outlet, such as a river or stream. It helps in understanding surface runoff dynamics, with shorter flow lengths indicating quicker water accumulation in drainage outlets, potentially increasing flood risk. Calculated using Digital Elevation Models (DEMs) in GIS software, flow length is integrated with other factors like slope and land use to create comprehensive flood hazard maps. This analysis aids in identifying areas most vulnerable to flooding and informs flood risk management strategies.

### 3.3 precipitation

Rainfall data was collected from Indian Meteorological Department (IMD). In the process of rainfall data, the point data have been converted into grid data through the Inverse Distance Weighted (IDW) interpolation tool in ArcGIS 10.8.1. It is Average annual rainfall data for the period of 10 years from 2014 to 2023 and are reclassified into five classes shown in Fig. 5.

### 3.4 River Distance

Distance from the river is one of the most important factors in flood hazard mapping. As the distance increases, the elevation and slope becomes higher. Also, Stream is generally the lowest point of that particular region. As a result of this, areas far from the river are having lower vulnerability of flood occurrence. During floods, river banks get overflowed and submerge the dry land nearby the river. In this study we have classified distance from river in to five classes from very high (0 – 3019 m), high (3020 – 6157 m), moderate (6158 – 11077 m), low (11078 – 14491 m), and very low (14492 – 51600) as shown in Fig.6. Lesser the distance from the river more is the flood vulnerability occurrence and more is the distance from the river lesser is the vulnerability.

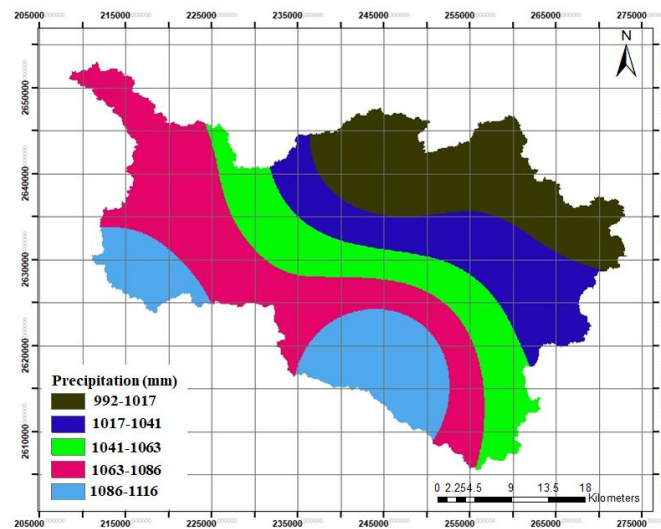


**Fig 5: Reclassified precipitation map**

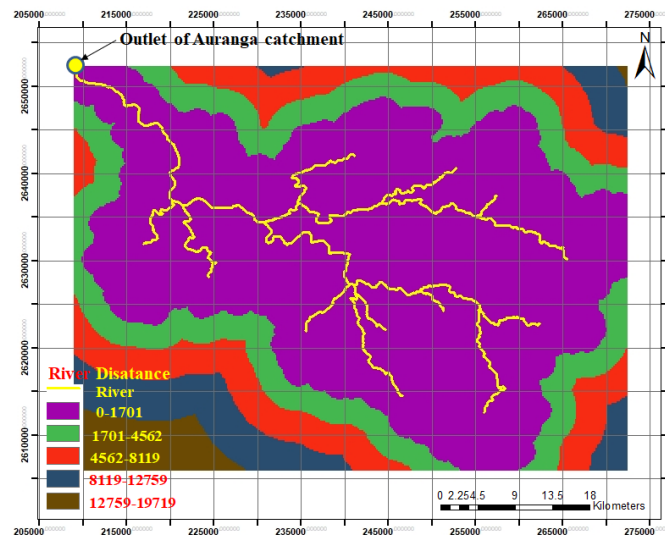


**Fig 6: Reclassified River distance map**

### 3.5 Land use /Land cover

Land Use-Land Cover (LU-LC) is the primary driver in changing the landscape of a specific area. LULC map has been downloaded from GlobCover web portal and are classified in to eleven classes, then further reclassified into five classes on the bases of weights such as class one Irrigation crop land / Rainfed crops having area of 922 km<sup>2</sup>, second class mosaic crop land / mosaic vegetation having area of 205 km<sup>2</sup>, third class evergreen forest/deciduous forest/built-up area of 256 km<sup>2</sup>, fourth class water bodies having area of 7 km<sup>2</sup>, and fifth class Shrubland/grassland having area of 164 km<sup>2</sup>. The study highlighted that the class third, fourth and fifth are regarded as highly susceptible, while class first and second are least vulnerable to flood as shown in Fig.7.

### 3.6 Elevation

In the study of flood hazard mapping, according to the expert’s opinion, the elevation of an area is the most important factor for controlling the flood vulnerability [32,33]. Regions located in higher elevation generally have the lower potentiality to be flooded, whereas lower elevated regions are having higher vulnerability potential. Water is having the tendency to flow towards the lower region from a higher region; and therefore, low elevated regions with a flat surface area have a higher potential of flood



occurrences [30]. The elevation of the study area ranges from 226 to 1090 m and reclassified into 5 classes as shown in Fig. 8.

#### 4.0 Assessment of flood Hazard Mapping Zones

The resultant flood susceptibility map exhibits values, ranging from 135 to 465, are categorized into five distinctive classes, using the natural breaking method in ArcGIS 10.8.1 as shown in Fig.11. The classes are very low, Low, moderate, high and very high probability of flood comprising 6.4%, 12.7%, 20.8%, 35.9%, and 24.2%. And are having the area of 97 km<sup>2</sup>, 193 km<sup>2</sup>, 316 km<sup>2</sup>, 545 km<sup>2</sup>, and 369 km<sup>2</sup> of the study area shown in Figures 9 and 10 respectively and Table 4.

The areas with very high flood hazard places are located on both sides of the Auranga River. Some of these places, such as Demu, Dhankara, Bhusur, Narayanpur, and Murmu, are situated at higher elevations in the Auranga River catchment. Further downstream, in the middle section of the catchment, are locations like Ledhpa, Godhna, Bendi, Deobar, Udaipur, and Karhuma. As we move towards the lower elevations downstream, the areas prone to severe flooding include Putki, Hosir, Jeruna, Kope, Simri, Sisi, Palamu Fort, Manasoti, Pokhro Khurd, Kamaru, Palpol Kalan, and Lukumkhar.

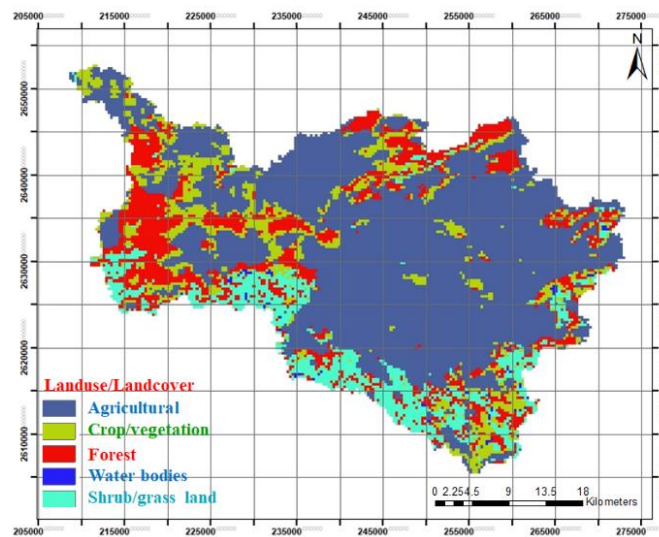


**Fig. 7: Reclassified Landuse/Landcover Map**

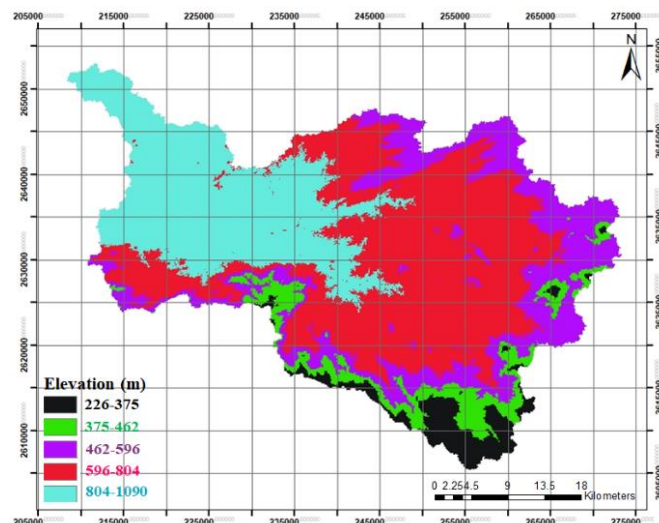


**Fig. 8: Reclassified Elevation Map**

Approximately 545 square kilometers of land are classified as high flood hazard zones, posing significant risks during heavy rainfall or river flooding. This extensive area includes several vulnerable locations, such as Barwakhar, Chandwa, Sasang, Surdi, Lejang, Latehar, and Matlaung. These areas are particularly prone to flooding due to their geographic characteristics, proximity to water bodies, and terrain features that make them susceptible to water overflow.

The moderate flood hazard zone spans an area of approximately 316 square kilometers, encompassing several regions that are moderately vulnerable to flooding during periods of intense rainfall or river overflow. Notable areas within this zone include Lath Dam, Bankita, Meral, Pakri, Balu, and Alaudi. While these areas do not face the same level of flood risk as high hazard zones, they are still susceptible to flooding that can disrupt local infrastructure, agriculture, and daily life. The moderate flood hazard designation indicates that these regions may experience occasional flooding, which can result in temporary waterlogging, damage to crops, and challenges in transportation. Proactive measures such as improved drainage systems, flood preparedness, and community awareness are essential for reducing the potential impact on these moderately at-risk areas.

The very low and low flood hazard zones are located farther from the Auranga River catchment, as indicated on the flood hazard zone map. These zones cover an area of approximately 290 square kilometers, including locations such as Salaiya, Gorpat, Lawapani, Bairobar, Uldag, Bingara, Bikra, and parts of the Gotang and Chatuang forest areas, which are situated at higher elevations within the Auranga catchment. These regions face minimal risk of flooding due to their distance from the river and elevated terrain, making them less susceptible to water overflow during heavy rains. While these areas are generally safe from flood hazards, they still benefit from monitoring and preparedness, especially in the event of extreme weather conditions.

**Table 4: Flood Hazard Zone area and percentage**

Flood Hazard Zone	Area in Km <sup>2</sup>	Area in (%)
Very Low	97	6.4
Low	193	12.7
Moderate	316	20.8
High	545	35.9
Very High	369	24.2
Total sum	1520	100%

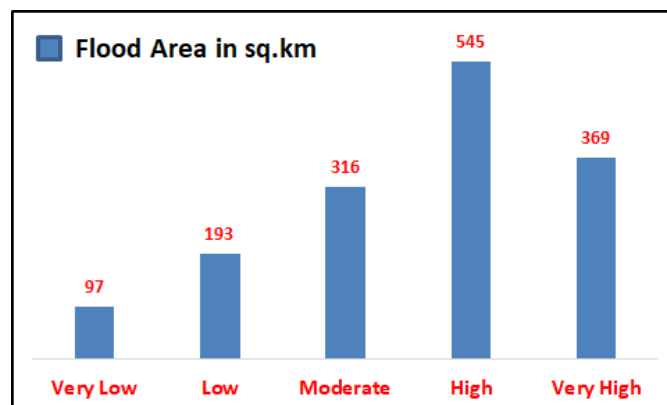


**Figure 9: Flood Area in sq.km**

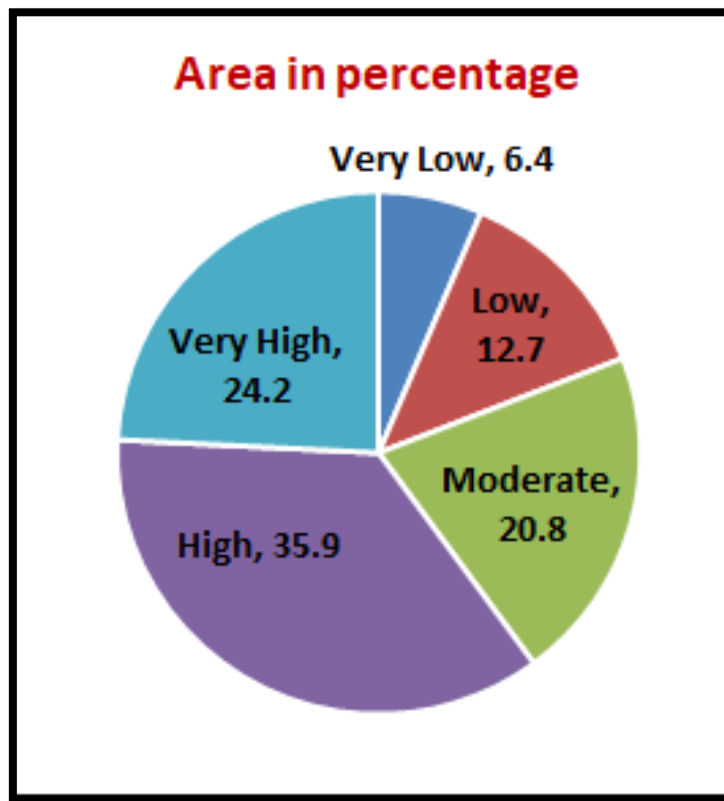


**Figure 10: Flood Area in percentage**

About 20.8% area in the study area shows moderate susceptibility of flood. These locations are mostly agricultural along the coastal rivers and water bodies are very high, and moderately affected, north-eastern part of the study area having lower elevation and slope, and are more susceptible for water accumulation, because of its topography, are more vulnerable to floods.

The Southern and south eastern part of the study area is less vulnerable than north eastern part because of its steep slope and slight high elevation than the north-western part of the study area. In this area the streams to have high velocity, which cannot allow the water to accumulate in this regions, consequently, these regions shows very low flood vulnerability.

Moreover, the flood susceptibility through geospatial mapping can be improved by the selection of high-resolution spatial datasets [34]. accurate convention data, and an advance the accuracy by comparing the results, and it will helps the decision makers and administrative bodies in achieving proper planning and management. Although floods are not very catastrophic in this region, but on the other hand cause measurable demerges to the agricultural activities. The regions identified as high flood zone (HFZ) require some serious attention of the administrative bodies to prevent flood conditions in future.

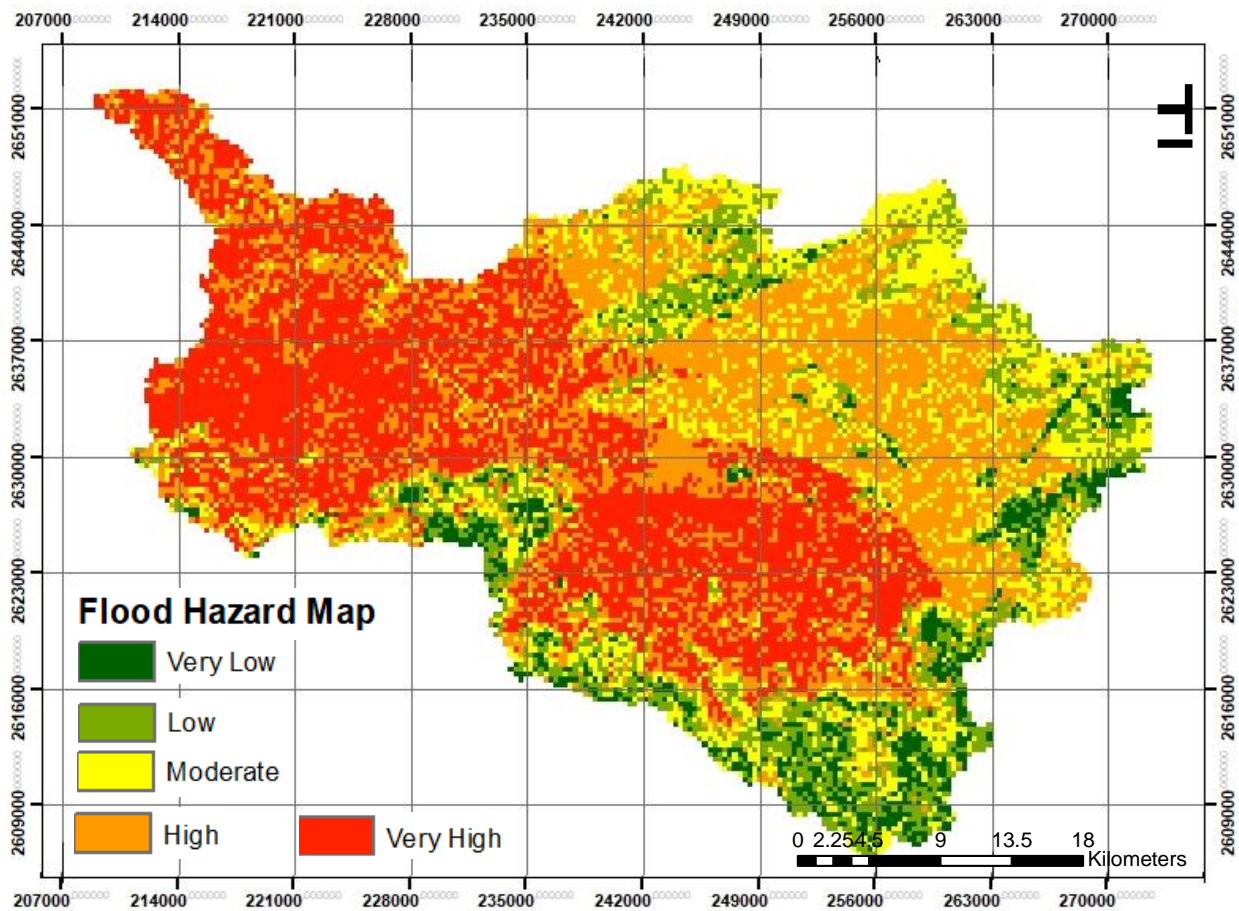


**Figure 11: Flood Hazard Zone Map of Auranga Watershed**

Previously, several studies are carried out in the different places around the world to build an accurate flood susceptibility map using several decision- making and machine learning approaches. Kaur et al. [35] employed Yule’s (1912) coefficient model through Weighted Overlay Analysis in GIS to predict possible flood susceptible regions in West Bengal, India. Prediction of flood using this method offered quite an accurate result. Similar methods are adapted by many researchers to assess hazard zonation using geospatial modeling [36,37]. Risi et al. [38] carried out flood predication analysis by assessment of TWI and maximum likelihood modeling. In the present study, it is seen that elevation, slope, and rainfall are the most important parameters for the assessment of flood hazard.

In current times, planners from different places of the world emphasized the significance of decision-making approaches through GIS techniques in flood susceptible zonation, which is very cost-time-effective. The accuracy of the Weighted Overlay analysis (WOA) technique depends on assigned weights. However, the significant point is that in different studies it is observed a inequality in weightage and ranking given for a certain parameter by different researchers. The attempt to prepare precise flood hazard map depends on the data accessibility of different parameters, accuracy, and regional conditions.

## 5. Conclusions

The present study identifying the flood hazard zones, as a prerequisite approach in demarcating the degree of susceptibility of various regions towards the natural calamity. Being the most efficient and widely acceptable techniques, MCDM-based Weighted Overlay Analysis (WOA) model approach was carrying



out the flood hazard analysis of the Auranga catchment of Latehar District of Jharkhand state. The research has been conducted by utilizing WOA and geospatial techniques that provided a cost-effective and less time-consuming methodology. Numerous factors such as elevation, slope, rainfall, Landuse/Landover, distance from river, and flow length maps are integrated in the ArcGIS platform. As a result, a flood hazard map has been produced, which shows that about 24.2% of the total study area is having very high, 35.9% high, 20.8% moderate, 12.7% low, and 6.4% very low respectively. These regions are mostly located near southern and western parts of the study area along the North Koel River. These regions are requiring some serious attention of governmental and local bodies to reduce the flood risk. This current study will be a very useful tool for the policy planners and coastal management planners to make effective decisions towards mitigation measures in flood prone areas in the Auranga catchment.

## References

1. Giordan, D.; Notti, D.; Villa, A.; Zucca, F.; Calo, F.; Pepe, A. Low cost, multiscale and multi-sensor application for flooded area mapping. *Nat. Hazards Earth Syst. Sci.* 2018, 18, 1493–1516. [[CrossRef](#)]
2. Sofia, G.; Roder, G.; Dalla Fontana, G.; Tarolli, P. Flood dynamics in urbanised landscapes: 100 years of climate and humans' interaction. *Sci. Rep.* 2017, 7, 40527. [[CrossRef](#)] [[PubMed](#)]
3. Smith, A.; Bates, P.D.; Wing, O.; Sampson, C.; Quinn, N.; Neal, J. New estimates of flood exposure in developing countries using high-resolution population data. *Nat. Commun.* 2019, 10, 1814. [[CrossRef](#)] [[PubMed](#)]
4. Souissi, D.; Zouhri, L.; Hammami, S.; Msaddek, M.H.; Zghibi, A.; Dlala, M. GIS-based MCDM-AHP modeling for flood susceptibility mapping of arid areas, southeastern Tunisia. *Geocarto Int.* 2019, 35, 991–1017. [[CrossRef](#)]
5. Pradhan, B. Flood susceptible mapping and risk area delineation using logistic regression, GIS and Remote sensing. *J. Spat. Hydrol.* 2009, 9, 1–18.
6. Siahkamari, S.; Haghizadeh, A.; Zeinivand, H.; Tahmasebipour, N.; Rahmati, O. Spatial prediction of flood-susceptible areas using frequency ratio and maximum entropy models. *Geocarto Int.* 2018, 33, 927–941. [[CrossRef](#)]
7. Shafapour-Tehrany, M.; Shabani, F.; NeamahJebur, M.; Hong, H.; Pourghasemi, H.R.; Xie, X. GIS-based spatial prediction of flood prone areas using standalone frequency ratio, logistic regression, weight of evidence and their ensemble techniques. *Geomat. Nat. Hazards Risk* 2017, 8, 1538–1561. [[CrossRef](#)]
8. Liu, K.; Li, Z.; Yao, C.; Chen, J.; Zhang, K.; Saifullah, M. Coupling the k-nearest neighbor procedure with the Kalman filter for real-time updating of the hydraulic model in flood forecasting. *Int. J. Sediment Res.* 2016, 31, 149–158. [[CrossRef](#)]
9. Dano, U.; Balogun, A.L.; Matori, A.N.; Wan Yusouf, K.; Rimi Abubakar, I.; Said Mohamed, M.; Pradhan, B. Flood Susceptibility Mapping Using GIS-Based Analytic Network Process: A Case Study of Perlis, Malaysia. *Water* 2019, 11, 615. [[CrossRef](#)]
10. Li, Y.; Martinis, S.; Wieland, M.; Schlaer, S.; Natsuaki, R. Urban Flood Mapping Using SAR Intensity and Interferometric Coherence via Bayesian Network Fusion. *Remote Sens.* 2019, 11, 2231. [[CrossRef](#)]
11. Rahmati, O.; Zeinivand, H.; Besharat, M. Flood hazard zoning in Yasooj region, Iran, using GIS and multi-criteria decision analysis. *Geomat. Nat. Hazards Risk* 2016, 7, 1000–1017. [[CrossRef](#)]



12. Oeurng, C.; Sauvage, S.; Sánchez-Pérez, J.M. Assessment of hydrology, sediment and particulate organic carbon yield in a large agricultural catchment using the SWAT model. *J. Hydrol.* 2011, 401, 145–153. [[CrossRef](#)]
13. Choubin, B.; Moradi, E.; Golshan, M.; Adamowski, J.; Sajedi-Hosseini, F.; Mosavi, A. An ensemble prediction of flood susceptibility using multivariate discriminant analysis, classification and regression trees, and support vector machines. *Sci. Total Environ.* 2019, 651, 2087–2096. [[CrossRef](#)]
14. Hong, H.; Tsangaratos, P.; Ilija, I.; Liu, J.; Zhu, A.X.; Chen, W. Application of fuzzy weight of evidence and data mining techniques in construction of flood susceptibility map of Poyang County, China. *Sci. Total Environ.* 2018, 625, 575–588. [[CrossRef](#)]
15. Khosravi, K.; Pham, B.T.; Chapi, K.; Shirzadi, A.; Shahabi, H.; Revhaug, I.; Prakash, I.; Bui, D.T. A comparative assessment of decision trees algorithms for flash flood susceptibility modeling at Haraz watershed, Northern Iran. *Sci. Total Environ.* 2018, 627, 744–755. [[CrossRef](#)]
16. Wang, Y.; Fang, Z.; Hong, H.; Peng, L. Flood susceptibility mapping using convolutional neural network frameworks. *J. Hydrol.* 2020, 582, 124482. [[CrossRef](#)]
17. Jahangir, M.H.; Reineh, S.M.M.; Abolghasemi, M. Spatial predication of flood zonation mapping in Kan River Basin, Iran, using artificial neural network algorithm. *Weather Clim. Extrem.* 2019, 25, 100215. [[CrossRef](#)]
18. Duan, Q.; Sorooshian, S.; Gupta, V. E\_ective and e\_icient global optimization for conceptual rainfall-runoff models. *Water Resour. Res.* 1992, 28, 1015–1031. [[CrossRef](#)]
19. Bahrami, S. Global Ensemble Stream Flow and Flood Modeling with Application of Large Data Analytics, Deep Learning and GIS. Unpublished Master's Thesis, University of Nevada, Reno, NV, USA, 2019; p. 210.
20. Tellman, B.; Kuhn, C.; Max, S.A.; Sullivan, J. Dynamic Flood Vulnerability Mapping with Google Earth Engine. In *Proceedings of the American Geophysical Union Fall Meeting, San Francisco, CA, USA, 14–18 December 2015*; pp. 5523–5527.
21. Liu, C.C.; Shieh, M.C.; Ke, M.S.; Wang, K.H. Flood Prevention and Emergency Response System Powered by Google Earth Engine. *Remote Sens.* 2018, 10, 1283. [[CrossRef](#)]
22. Hennessey, KJ, Gregory, JM & Mitchell, JFB 1997, „Changes in daily precipitation under enhanced greenhouse conditions“, *Climate Dynamics*, vol. 13, pp. 667–680. <https://doi.org/10.1186/s40677-016-0044-y>
23. IPCC (Intergovernmental Panel on Climate Change) (2007), *Climate Change 2007: The physical science basis. Contribution of working group I to the fourth assessment report of the intergovernmental panel on climate change*, edited by Solomon, S *et al.*, Cambridge Univ. Press.
24. Vojtek, M.; Vojteková, J. Flood Susceptibility Mapping on a National Scale in Slovakia Using the Analytical Hierarchy Process. *Water* 2019, 11, 364. [[CrossRef](#)]
25. GhorbaniNejad, S.; Falah, F.; Daneshfar, M.; Haghizadeh, A.; Rahmati, O. Delineation of groundwater potential zones using remote sensing and GIS-based data-driven models. *Geocarto Int.* 2017, 32, 167–187.
26. Beven, K.J.; Kirkby, M.J.A. Physically based, variable contributing area model of basin hydrology/Un modèle à base physique de zone d'appel variable de l'hydrologie du bassin versant. *Hydrol. Sci. J.* 1979, 24, 43–69. [[CrossRef](#)]
27. Bilskie, M.V.; Hagen, S.C.; Medeiros, S.C.; Passeri, D.L. Dynamics of sea level rise and coastal flooding on a changing landscape. *Geophys. Res. Lett.* 2014, 41, 927–934. [[CrossRef](#)]

28. Lim J, Lee K (2017) Investigating flood susceptible areas in inaccessible regions using remote sensing and geographic information system. *Environ Monit Assess* 189:96
29. Mojaddadi H, Pradhan B, Nampak H, Ahmad N, Ghazali AHB (2017) Ensemble machine learning-based geospatial approach for flood risk assessment using multi-sensor remote sensing data and GIS. *Geomatics Nat Hazard Risk* 8:1080–1102.
30. Das S, Pardeshi SD, Kulkarni PP, Doke A (2018) Extraction of lineaments from different azimuth angles using geospatial techniques: a case study of Pravara basin, Maharashtra, India. *Arab J Geosci* 11: 160. <https://doi.org/10.1007/s12517-018-3522-6>.
31. Masoudian, M., 2009. The topographical impact on effectiveness of flood protection measures (Ph.D. thesis). Faculty of Civil Engineering, Kassel University, Germany. <http://www.uni-kassel.de/upress/online/frei/978-3-89958-790-6.volltext.frei>.
32. Botzen WJW, Aerts JCJH, van den Bergh CJM (2012) Individual preferences for reducing flood risk to near zero through elevation. *Mitig Adapt Strateg Glob Change* (2):229–244. <https://doi.org/10.1007/s11027-012-9359-5>.
33. Pradhan B (2009), Groundwater potential zonation for basaltic watersheds using satellite remote sensing data and GIS techniques. *Open Geosci* 1:120–129. <https://doi.org/10.2478/v10085-009-0008-5>
34. Senanayake IP, Dissanayake DMDOK, Mayadunna BB, Weerasekera WL (2016) An approach to delineate groundwater recharge potential sites in Ambalantota, Sri Lanka using GIS techniques. *Geosci Fron* 7:115–124
35. Kaur H, Gupta S, Prakash S, Thapa R, Mandal R (2017) Geospatial modelling of flood susceptibility pattern in a subtropical area of Khole, M & De, US 2001, „Socio-economic impacts of natural disasters“, WMO. Bulletin, vol. 50, pp. 35–40.
36. Bonham-Carter GF (1994) *Geographic information systems for geoscientists: modeling with GIS*. Pergamon, Elsevier Science Ltd, p 398.
37. Ghosh S, Carranza EJM, Van-Westen CJ, Jetten VG, Bhattacharya DN (2011) Selecting and weighting spatial predictors for empirical modeling of landslide susceptibility in the Darjeeling Himalayas (India). *Geomorphology* 131:35–56.
38. Risi RD, Jalayer F, Paola FD, Lindley S (2017) Delineation of flooding risk hotspot based on digital elevation model, calculated and historical flooding extents: the case of Ouagadougou. *Stoch Environ Res Risk Assess*. 32:1545–1559. <https://doi.org/10.1007/s00477-017-1450-8>

Licensed under [Creative Commons Attribution-ShareAlike 4.0 International License](https://creativecommons.org/licenses/by-sa/4.0/)